Computer modelled internal pressure strength predictions for refillable glass containers[1])

By Bengt O. Augustsson, Hammar (Sweden); John S. Wasylyk and Russell D. Southwick, Butler, PA (USA)

(Communication of the PLM Glass Research and Development, Hammar (Sweden), and American Glass Research, Inc., Butler, PA (USA))

(Received 18 June 1985)

The strength of a glass container under different types of loads will be determined by several interrelated factors. Varying stresses will be produced at different locations on a bottle surface when loads are applied to the bottle, due to different bottle shapes, wall thicknesses and wall thickness variations. This study provides a method which may be used to describe the stress and strength at each location on a glass container surface, and also provide a fracture strength distribution for certain types of loads.

Modèle informatique pour prévoir la résistance des récipients en verre

La résistance d'un récipient en verre soumis à différents types de sollicitations, est déterminée par plusieurs facteurs interdépendants. Des contraintes différentes apparaissent à divers endroits d'une surface de bouteille lorsque celle-ci est soumise à des contraintes dues à différentes formes de bouteille, d'épaisseur de verre et à des variations d'épaisseur de paroi. Cette étude qui utilise un modèle informatique, offre une méthode qui décrit les contraintes et la résistance mécanique pour chaque point d'une surface de récipient en verre et qui permet de connaître la répartition de la résistance à la rupture pour des types de sollicitations déterminés.

Computermodell zur Voraussage der Festigkeit von Glasbehältern

Die Festigkeit eines Glasbehälters bei unterschiedlichen Arten von Belastungen wird von mehreren, miteinander in Zusammenhang stehenden Faktoren bestimmt. Unterschiedliche Spannungen entstehen an verschiedenen Stellen einer Flaschenoberfläche, wenn eine Flasche Belastungen ausgesetzt wird, bedingt durch unterschiedliche Flaschenformen, Wanddicken und Wanddickenschwankungen. Die Untersuchung an Hand des Computermodells bietet eine Methode der Spannungs- und Festigkeitsbeschreibung für jeden Punkt einer Glasbehälteroberfläche und ermöglicht es, die Bruchfestigkeitsverteilung bei bestimmten Belastungsarten zu erkennen.

1. Introduction

The strength of a glass container subjected to a given load is determined by several interrelated factors. Bottle shape, absolute wall thickness and wall thickness variations with location on the bottle surface will give varying types and magnitudes of stress at different locations on the bottle wall when different loads are applied to the bottle. The fracture stress or strength at each particular location on the bottle surface will also vary, and will also be determined by the type or nature of each discontinuity and the magnitude of the depth of each of the discontinuities present on the glass surface. When the applied load is increased to the point of failure, different failure load levels will be obtained for different containers due to the different stresses generated on each container. The resultant strengths obtained for each individual container will also be different, accordingly. The stresses generated at each location of the container may be estimated as a function of the applied load, container shape, wall thickness and variation in wall thickness. The fracture stress at each location on the bottle can also be estimated as a function of the surface discontinuity size, discontinuity type and frequency of occurrence which results from the manufacturing process, and the subsequent handling of the container. The largest ratio between generated stress due to applied load and fracture stress determined by surface discontinuities found at any location on the container surface, will then determine both the strength, and the location of the fracture origin of any one container.

This study will detail a procedure which may be used to predict the internal pressure stresses and strengths at each location on a refillable bottle, and to also obtain a resulting pressure strength distribution for an internal pressure load applied to that same bottle. The predictive method requires prior knowledge of variations in the respective glass thickness and surface discontinuity distributions. Such variations and distributions will be characteristic of any particular manufacturing process and subsequent bottle handling system. The analysis also requires prior knowledge of the relationship between the

[1]) Presented to the 59th Conference of the German Glass Technology Society in Bad Homburg on 22th May 1985.

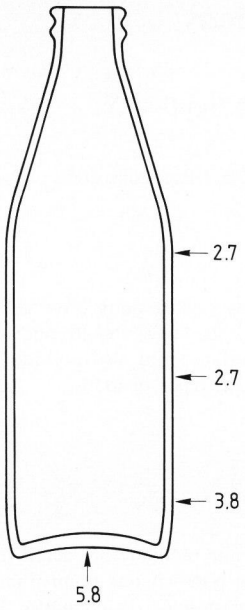

Figure 1. The 33 cl bottle design used in the predictive strength model. Numbers refer to average thicknesses in mm measured at the indicated locations on the bottle surface.

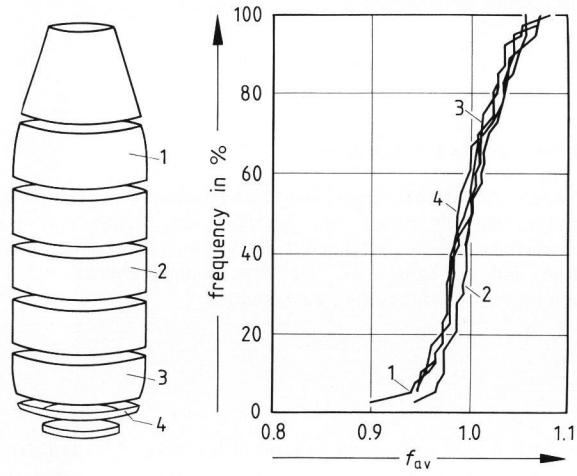

Figure 3. Average thickness distributions in indicated representative segments of 33 cl bottle.

applied pressure load and the resultant pressure stresses which are obtained for different locations on the surface of a given container design. Such analyses may be readily obtained either from experience, experiment, or from the many different types of computer finite element stress analysis packages, now available.

The method described herein also provides a useful tool for predicting pressure strengths for a given refillable bottle design and manufacturing process. The method also offers a means of optimizing the container design for specific strength requirements.

It is obvious that there are difficulties in obtaining reproducible information regarding surface damage distributions for the sizes and amounts of such damage for nonrefillable containers. The lack of reproducibility is due primarily to variations in hot end handling and surface coating quality. Refillable

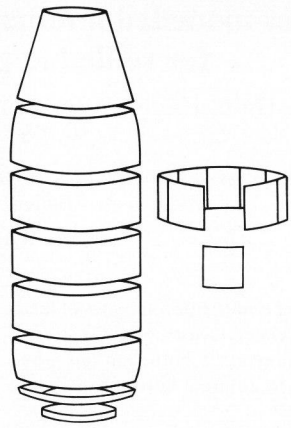

Figure 2. Segmentation scheme of 33 cl bottles used in strength prediction study.

bottles offer a more likely prospect of being able to determine specific surface discontinuity distributions after repeated usage. But the method also holds significant promise for continued development and application to nonrefillable containers as well.

2. Container design used in model

The particular container design used in this study was a refillable bottle of 33 cl (10 U.S. fluid ounce) capacity, as seen in figure 1. Also shown in that figure is an illustration of the average thickness distribution obtained from a representative sampling of similar bottles. Based on the expected fracture origin locations and shape of the container, the bottle was divided into a limited number of circular segments as shown in figure 2. Each segment was then divided into a further limited number of rectangular divisions. The bottle is then described by a limited number of elements, each having a size determined by the expected variation in wall thickness, bottle shape and surface discontinuity distribution.

3. Wall thickness variation

Due to variations inherent in the forming process, the wall thickness in each segment of a bottle will be different for each individual container studied. The thickness will show distinct patterns of variation when measured in either the circumferential or longitudinal directions.

The average thickness variation from bottle to bottle within a given segment was examined first. The variations in average segment thickness $t_{av}(\text{seg})$ with respect to the calculated grand average thickness $t_{cav}(\text{seg})$ for a given segment has been studied for one instance of the blow and blow process. That variation can be expressed by $f_{av}(\text{seg})$, the ratio between the individual average segment thickness $t_{av}(\text{seg})$, and the calculated average thickness $t_{cav}(\text{seg})$ as follows:

$$f_{av}(\text{seg}) = t_{av}(\text{seg})/t_{cav}(\text{seg}) \,. \qquad (1)$$

An example of the distribution of the ratio $f_{av}(\text{seg})$ for different segments is shown in figure 3. Those data

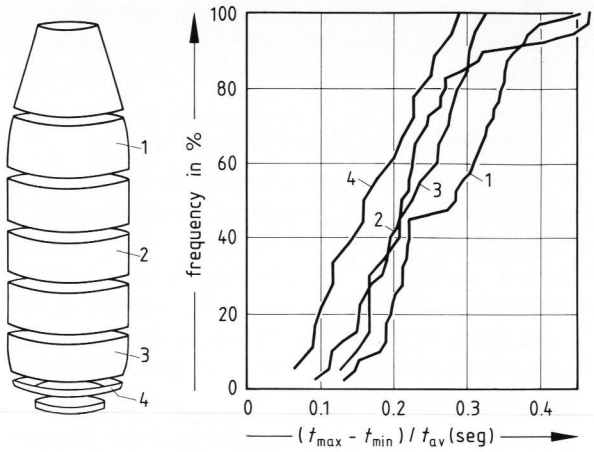

Figure 4. Variation of f_c(seg), relative range of circumferential wall thickness variation, in 33 cl bottle.

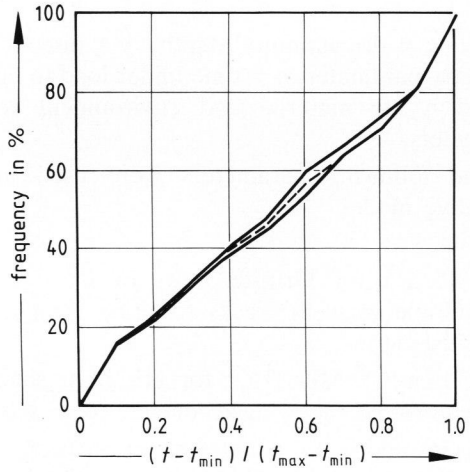

Figure 5. Distribution of f_t, relative deviation from minimum circumferential wall thickness (72 bottles; upper, middle and lower sidewall).

show a tendency to be grouped within ±10 % of the nominal unit value.

The variation of wall thickness in the circumferential direction has also been studied, and may be described by the ratio f_c(seg). The f_c(seg) ratio expresses circumferential thickness variations in terms of t_{max}, the largest, t_{min}, the smallest, and the average segment wall thickness t_{av}(seg) for a specified segment of a container as follows:

$$f_c(\text{seg}) = (t_{max} - t_{min})/t_{av}(\text{seg}) \; . \qquad (2)$$

The f_c(seg) ratio then determined the relative range of variation in circumferential glass thickness for each segment. Measured data are listed in figure 4. Those data show the measured f_c(seg) distribution for four different segments taken from the exemplar bottles.

The variation of glass thickness f_t between the indicated minimum and maximum values has also been studied for a large number of bottles, and is expressed as follows:

$$f_t = (t - t_{min})/(t_{max} - t_{min}) \; . \qquad (3)$$

The functional relationship can be seen by the data shown in figure 5. The data show that the individual thickness values t, measured throughout the upper, middle and lower bottle sidewall regions for 72 bottles, are not equally distributed between the maximum and minimum thickness values. The same distribution is obtained when two concentric cylinders are slightly displaced with respect to their centers.

Given the indicated functional relationship f_t above, and assuming that the value of $((t_{max} + t_{min})/t_{av}(\text{seg}))$ is approximately equal to 2, the wall thickness in each segment and the wall thickness in a division within a segment can be described for each bottle by the following relation for t(seg,div):

$$t(\text{seg,div}) = t_{cav}(\text{seg}) \cdot f_{av}(\text{seg}) \cdot \\ \cdot (1 - f_c(\text{seg}) \cdot (0.5 - f_t)) \; . \qquad (4)$$

Values for f_{av}(seg), f_c(seg) and f_t are randomly generated in the computer strength prediction model.

The distributions for f_{av}(seg) and f_c(seg) may be mathematically expressed in the form:

$$f(x) = U + \exp((\log(\log(1/(1 - x))) - A)/B) \; . (5)$$

The distribution for the function f_t may be further modelled by an expression of the form:

$$f(x) = 1 - 1/\exp(\exp(A + B \cdot \log(x - U))) \; , \quad (6)$$

in which A, B and U are constants which are characteristic of each particular distribution modelled.

4. Wall thickness–stress relation

In using the above described model for the prediction of the wall thickness t(seg,div) of each element or division within a segment of the container, a further assumption must be made. That assumption is that the corresponding circumferential pressure stresses are directly related to the wall thickness at each location.

To determine fully the nature of the relation between wall thickness and induced pressure stress, a finite element stress analysis was performed for internal pressure loading on three selected bottles of identical style. Each bottle possessed relatively large variations in wall thickness. The relationship between local circumferential pressure stress S and the average circumferential pressure stress S_0 for different seg-

ments of the bottle was determined as functions of the average wall thickness t_0, and the corresponding local wall thickness t, as seen in figure 6. The circumferential pressure stresses induced in the bottle sidewall by the internal pressure load are seen to be directly related to the local wall thickness t. The variability in the relative circumferential stress ratio S/S_0 increases as one passes through the bottle heel and bearing surface regions and on to the center bottom.

The local stress S(seg,div) is defined in this model to be given by the relationship:

$$S(\text{seg,div}) = (S_{\text{cav}}(\text{seg}) \cdot t_{\text{cav}}(\text{seg}))/t(\text{seg,div}) \; . \quad (7)$$

The above expression for S(seg,div) may be used to determine the circumferential pressure stresses in the bottle sidewall with greater accuracy than in the heel and bottom regions of the bottle, due to the simpler, essentially biaxial circumferential and longitudinal stress state in the relatively thin, cylindrical bottle sidewall.

S_{cav}(seg) is the largest calculated average pressure stress found within each segment as determined using finite element stress analysis methods. For example, the circumferential pressure stress is normally larger, by a factor of two, than the longitudinal pressure stress in the sidewall of a cylindrically shaped bottle.

For heavier-walled refillable bottles, internal pressure failures will normally occur in the shoulder contact region due to circumferential pressure stresses. Such failures will result in the shoulder contact region at sufficiently high internal pressure load levels due to the presence of handling discontinuities that are normally generated in that region after several trips through the trade. In that specific case, it would be possible to estimate the average circumferential pressure stress in the shoulder contact region directly from the bottle geometry, without having to resort to finite element analyses. The procedure for estimating the appropriate stress indices is given in section 5.

5. Surface damage–strength relation

The presence of a surface discontinuity at a specified location on a glass bottle surface uniquely determines the failure or fracture stress at the indicated location. The fracture stress may be expressed in terms of the size and geometry of the discontinuity, the chemical environment surrounding the discontinuity, and the time over which sufficient tensile loads are applied to the discontinuity.

The functional relationship between the fracture stress S_f and the above described parameters may be expressed as:

$$S_f = ((a_i)^{1-n/2})/(((n/2) - 1) \cdot C \cdot y^n \cdot t_f))^{(1/n)} \quad (8)$$

where: a_i = discontinuity depth, y = discontinuity geometry parameter, t_f = time under load to failure. C and n are material and environment related parameters.

The following parameters were used in the predictive model:

$n = 16.4$,

$y = 1.12 \cdot \sqrt{\pi}$ for Griffith flaws or $0.56 \cdot \sqrt{\pi}$ for multiple crescent cracks resulting from frictive translation,

$C = 1.714\ \text{m}^{1+n/2}\ \text{MPa}^{-n}\ \text{s}^{-1}$ for grit blast sharp indenter-type flaws, aged and tested in water.

The types, and hence geometries, of surface discontinuities may vary considerably on refillable and nonrefillable glass container surfaces. For example, surface discontinuities generated during the forming process will be each separately represented by characteristic fracture stress distributions. Such distributions have been determined for refillable and nonrefillable bottles sampled from production, as described later in section 7. The type of surface discontinuity formed on glass container surfaces following forming are more than likely to result from frictive contact of either glass or metal on the glass surface, producing the crescent shaped surface discontinuities shown in figure 7. The widths and depths of the crescent cracks are functions essentially of the shape of the frictively loaded contacting object, the

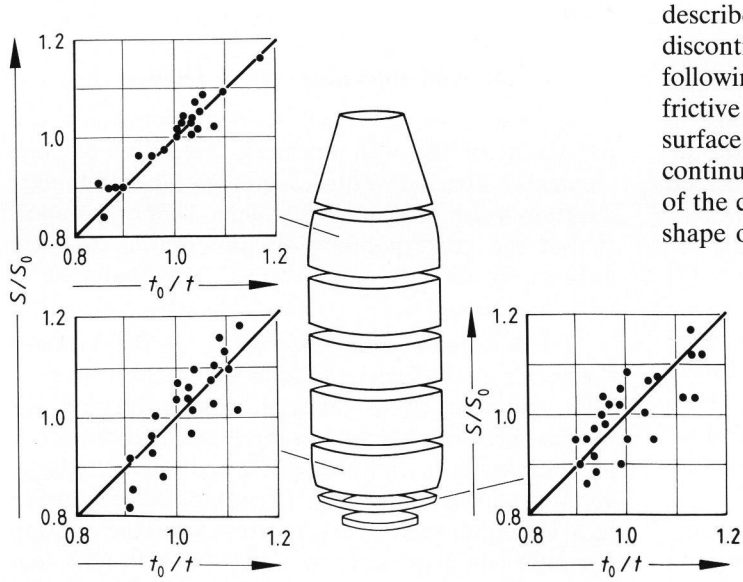

Figure 6. Linear relationship between local relative stress and average wall thickness deviation in the indicated segments.

force with which the contacting object bears on the surface, the elastic properties of both contacting objects, and the coefficient of friction between the contacting object and the contacted glass surface.

The crescent shaped discontinuities are not easily seen in an optical microscope. However, special surface preparation techniques such as hydrofluoric (HF) acid etching readily reveal the discontinuities, allowing their widths to be easily measured, as seen in figures 8a to c. Due to the relationship between the applied frictive load and the resulting contact stresses generated around the frictive loading object, measurements of crescent crack widths often show similar size distributions for different containers. The data shown in figures 9a to c reveal identical crescent crack width distributions for tin oxide coated and uncoated bottles of the same shape after having experienced several trips through a bottle filling line.

Although the widths w of crescent cracks may be easily measured as described above, the previously mentioned fracture equation requires the crack depth a_i, and not crack width w. Previous work [1] has been performed relating the depths of the frictively formed crescent cracks to the measured widths of the same discontinuities as measured on the original contacted surface. Those data, as shown in figures 10a and b, revealed a relatively constant measured crescent crack width to depth ratio of approximately four to one.

The technique used to measure the crescent crack depth data shown in figures 10a and b employed a physical measurement method. The remaining glass thickness was measured at a particular selected crescent crack location following HF acid etching. The surface etched was the glass surface opposite the originally contacted surface containing the crescent crack track.

Assuming that the same four to one ratio between crescent crack width and depth is valid for all hot-end frictive loading conditions, the value a_i in equation (8) may be replaced by $w/4$, in which w is the more easily determined crescent crack width resulting from

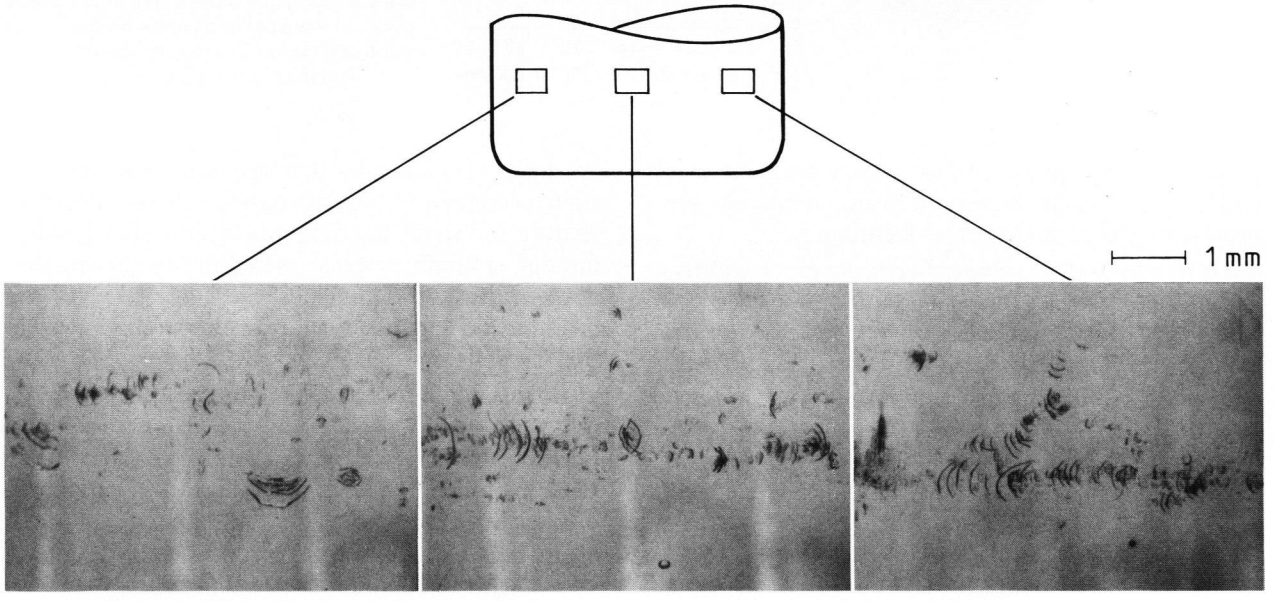

Figure 7. Three separate examples of types of frictive damage generated during use in heel contact zone of a British jam jar.

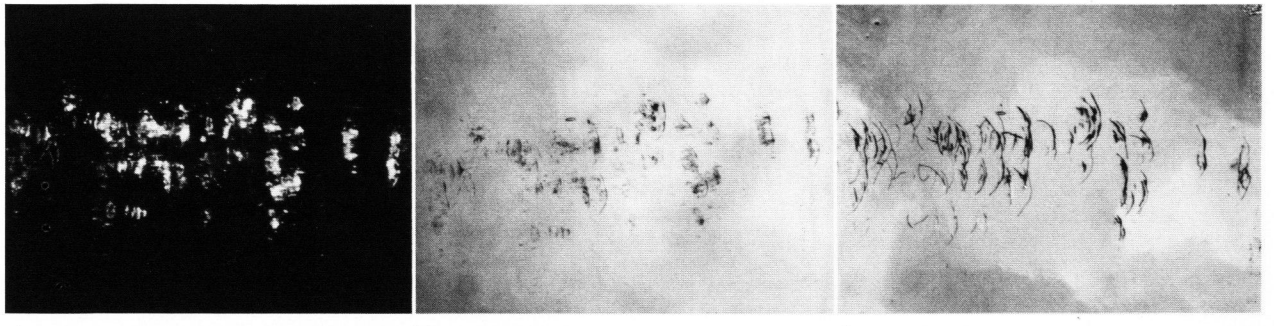

a) b) c)

Figures 8a to c. Optical microscope appearance of frictive damage on refillable bottles in a) reflected light, b) transmitted light, c) transmitted light following HF etching.

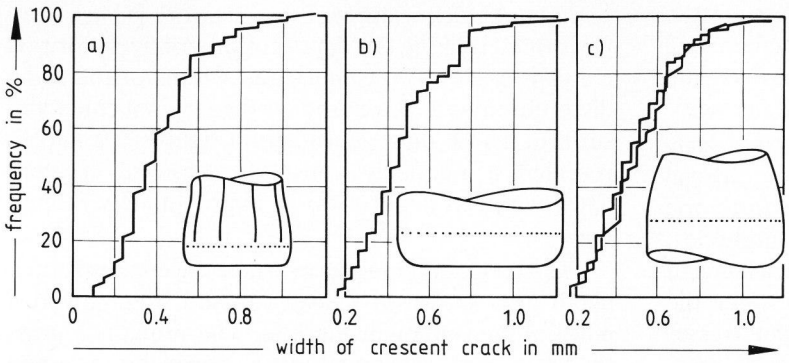

Figures 9a to c. Frictive damage crescent crack width frequency distributions measured on three different types of bottle, a) and b) uncoated, c) both uncoated and coated with tin oxide.

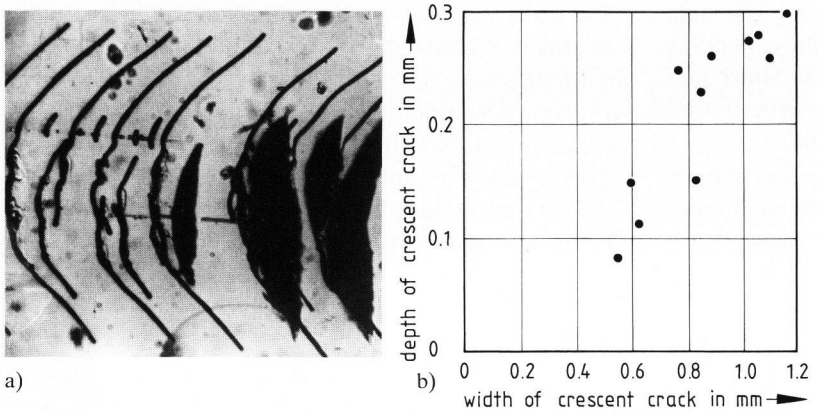

Figures 10a and b. Frictive damage crescent crack width measurement procedure and resultant depth/width relationship. a) Example of determination of crack depth by HF-etching. Dark spot indicates bottom of crescent crack. b) Example of relations between crack width and depth for crescent shaped discontinuities from sliding contact.

glass to glass frictive contact. Such crescent crack widths are readily measured using relatively low-powered optical microscope techniques.

Using measured values of crescent crack widths w in millimeters, and expressing the fracture stress S_f in terms of a one minute duration load, expressed in MPa as used in bottle pressure testing, the following relation is obtained for a simple half-penny shaped Griffith flaw:

$$S_f = 25.6 \cdot w^{-0.439} . \quad (9)$$

Data obtained for multiple crescent crack discontinuities, having a configuration different from Griffith flaws provides the relation:

$$S_f = 12.8 \cdot w^{-0.439} . \quad (10)$$

Earlier experimental work by Griffith indicated that the fracture stress of a brittle material such as glass should be proportional to the reciprocal square root of flaw depth. Using the Griffith relation and data from pressure strength determinations for a refillable bottle passing through a filling line 20 to 25 times, having a known internal pressure stress index at the shoulder contact region and a known surface frictive damage size distribution, the following relation for fracture stress S_f is obtained:

$$S_f = 17.2 \cdot w^{-0.5} . \quad (11)$$

Equation (11) indicates that strengths resulting from frictive crescent crack discontinuities will decrease sharply for small discontinuity widths, but reach a limiting strength value at increasing larger crescent crack widths. Equation (11) was then used as the basis for a computer-based pressure strength prediction model for refillable bottles.

Figure 11 shows the relation between internal pressure strengths converted to fracture stress as a function of crescent crack widths for the three separate functional relations listed in equations (9 through 11).

6. Strength predictive computer model

The computer model presently used to predict refillable glass container pressure strength distributions consists of two separate parts. The first part consists of a program module which is used to generate each of the separate wall thickness and surface discontinuity distributions used in the predictions. Each of the distributions is experimentally determined from calculated sets of constants A, B and U, a separate set of constants being used to statistically describe each particular discontinuity and wall thickness distributions. The second part of the program consists of a module which generates wall thickness and surface discontinuity distributions for each container style analyzed. The latter module also calculates the predicted strength distribution for a desired number of refillable containers.

The first part of the program requires the calculated largest average stress of each segment, normally obtained from a complete finite element stress analysis. However, refillable bottles will very often experience failure at the shoulder contact region on being pressure tested to sufficiently high levels of internal pressure. The relationship between the applied internal pressure load level and the circumferential pressure stress generated in the shoulder contact region can be expressed in terms of the bottle geometry at that location through the use of the thin wall boiler formula. The thin wall boiler formula may be used to calculate the circumferential and longitudinal pressure stresses in the outer wall surface of a long, cylindrically shaped vessel of uniform diameter and thickness. The boiler formula relates the larger stress in the circumferential direction on the bottle wall S_c generated by the applied internal pressure load P to a quantity termed the stress index, S_c/P expressed as follows:

$$S_c/P = D/(2\,t) \qquad (12)$$

where D is the cylinder diameter and t is the cylinder wall thickness.

For the purposes of the strength predictive model, the average wall thickness t_{av} at the shoulder contact segment may be used for t in equation (12). Values of the circumferential pressure stress index S_c/P are shown plotted against $D/(2\,t)$ in figure 12 for three different refillable bottle styles, having different ratios of shoulder radius to body diameter. The diagram shows the influence of the shoulder region radius on the circumferential pressure stress index found in the shoulder contact region. The data in figure 11 indicate that relatively simple geometrical considerations may be effectively substituted for more complex and expensive finite element analyses in determining shoulder contact region circumferential pressure stress indices for a given bottle style.

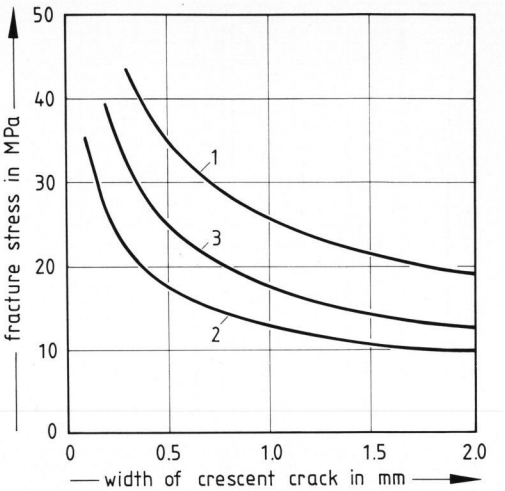

Figure 11. Fracture stress derived from internal pressure strength data as a function of frictive damage crescent crack width, according to three different functional relationships. Curve 1 represents equation (9), curve 2 equation (10), and curve 3 equation (11).

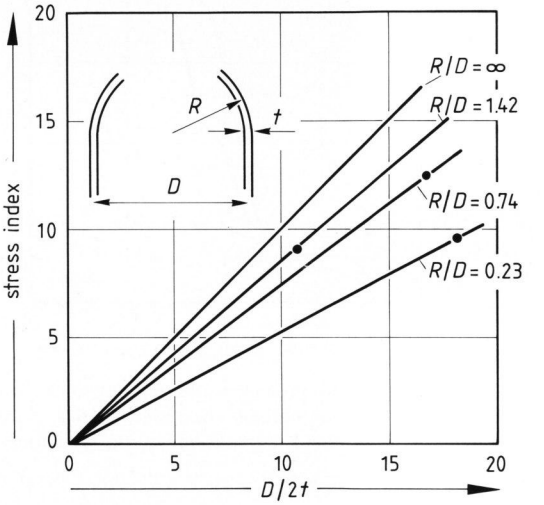

Figure 12. Differences in measured circumferential pressure stress index in the shoulder contact region for bottle styles having varying R/D, or shoulder contact radius R to body diameter D ratios, as functions of $D/2\,t$, geometrical pressure stress index.

7. Modelling surface discontinuities

The prediction of bottle pressure strengths at a point in time immediately following forming requires detailed knowledge of the many different possible types of surface discontinuities which may be produced during the forming process, and also the relationship between those discontinuities and their corresponding fracture stresses. It is obviously not possible to predict the frequencies and types of all possible kinds of discontinuities obtained in present day container forming processes. However, an example will serve to demonstrate the techniques which may be used to simulate a pressure strength distribution, should such information become readily available.

If, for example, the most severe types of discontinuity were to be eliminated from the forming process, the resulting improved pressure strength distribution could be studied by means of computer simulations, rather than empirical methods on the manufacturing shop floor. The following example represents data obtained for a 48 cl (16 fluid ounce) nonrefillable beverage bottle manufactured in an American container plant. The bottles were being produced on an eight section double-gob IS machine at a rate of approximately ten bottles per minute per cavity. Ten closely spaced rounds or 160 bottles were carefully sampled in sequence from the annealing lehr belt, immediately following application of the cold end coating material. The bottles were immediately pressure tested to destruction in an AGR ramp pressure tester. The pressure strengths and the

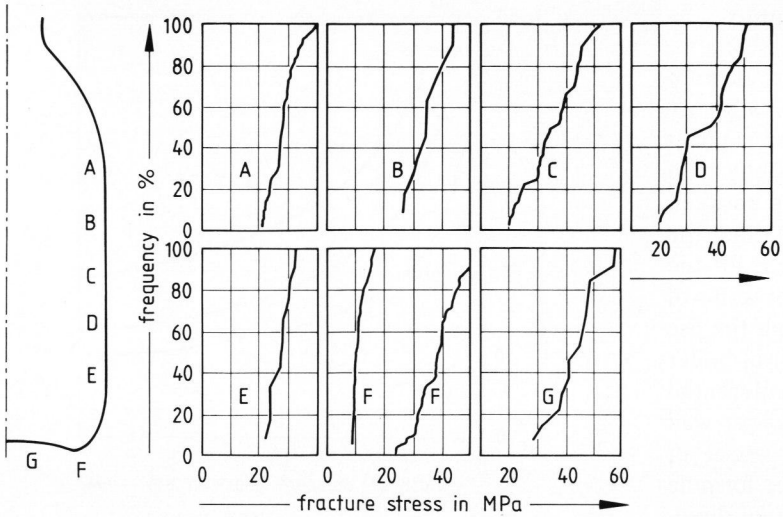

Figure 13. Fracture stress distributions due to internal pressure loading for the indicated fracture origin locations on the surface of a 48 cl nonrefillable American beverage bottle.

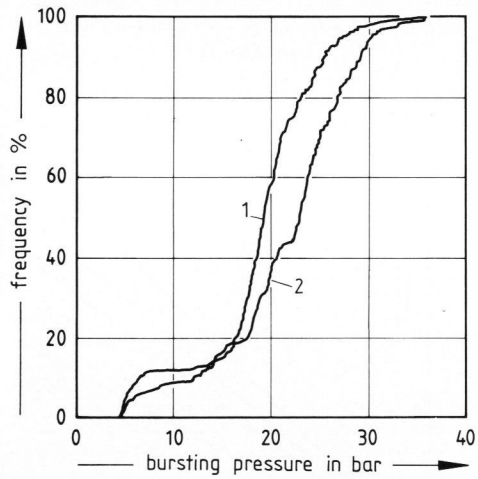

Figure 14. Measured and predicted internal pressure strength distributions for 48 cl nonrefillable beverage bottles. Curve 1: computer model calculated, curve 2: measured (200 bottles).

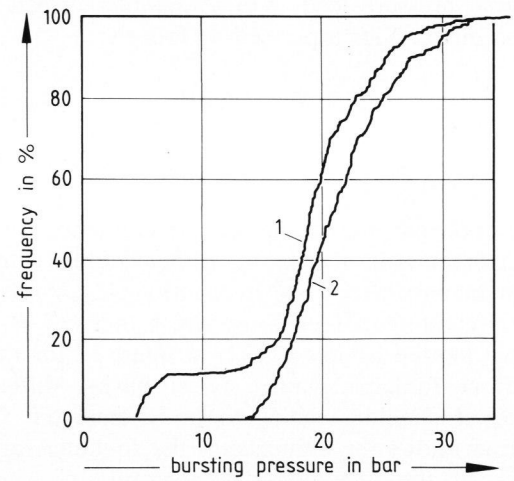

Figure 15. Internal pressure strength distribution resulting from elimination of bearing surface fracture origins (samples from lehr). Curve 1: original, curve 2: bearing surface discontinuities excluded.

fracture origin locations were recorded, and the fracture origins were saved for later microscopic examination and identification of the discontinuities at the fracture origins.

The pressure stress indices, or the functional relationship between the pressure stresses developed in the bottle walls and the applied internal pressure load for all locations on the bottle surfaces were determined by means of a proprietary finite element stress analysis program. The internal pressure strengths at failure, as obtained from the pressure tester, can then be converted to fracture stresses for each segment at each location on the bottle surface, given the locations and thicknesses of the individual fracture origins. The distributions of these fracture stresses are shown in figure 13. All segments analyzed evidenced fracture stress or strength distributions which were capable of being described in terms of a single statistical distribution, with the exception of the bottle bearing surface. That location showed two distinctly different strength distributions, seen as the two distributions both labeled F in figure 13. Two distinctly different strength distributions indicate that two different types of surface discontinuity were responsible for the pressure failures at the bearing surface location.

Knowing the total number of separate failure origin modes and the fracture stress or strength distribution in each segment, the overall pressure strength distribution for the specified conditions may then be determined using the computer model. The relation in equation (11) was used to express the fracture stress distribution in terms of the crescent crack width w. Figure 14 shows a comparison between the measured and computer predicted internal pressure strength distributions.

If, for example, both types of bearing surface discontinuity were to be eliminated from the parent pressure strength distribution, the remaining pressure strength distribution shown in figure 15 would result.

An increase in the minimum pressure strength is seen, as is an increase in the mean pressure strength for the resultant pressure strength distribution.

Statistical analyses of the individual origin mode data obtained for the nonrefillable bottle pressure strengths show the individual origin mode data capable of being described by a single distribution, with the exception of the bearing surface, as previously described. Microscopic examination of the origins at locations other than the bearing surface indicate more than one type of discontinuity to be present in each fracture stress population. It is not possible to obtain a general fracture stress distribution for each type of discontinuity capable of being produced during the forming operation. But the resultant strength data are clearly capable of being represented by representative single statistical distribution functions.

Discontinuities such as stones, seeds, thermal checks and infolds will result in tremendously large variations in their respective fracture stress distributions, due to the inherently large range in the sizes of each of the mentioned discontinuities. However, it is possible that discontinuities produced in the manufacturing plant hot-end due to frictive contact, shear scars, valve marks and inside surface discontinuities such as black specks will give more reproducible, and less variable, fracture stress distributions. Such distributions will lend themselves more readily to predictive modelling efforts.

It is likely that continuing determinations of fracture stress distributions for additional types of discontinuities will result in more accurate predictions of fracture stress distributions. The present model will of necessity need to be confined only to those situations in which fracture stress and surface discontinuity distributions may be accurately determined and hence predicted as for refillable bottles.

8. Example of internal pressure strength prediction

The predicted pressure strength data used in this study represent the particular European designed 33 cl refillable beverage bottle, shown previously in figure 1. Assuming that failure due to internal pressure loading will occur only in the upper shoulder contact region of the bottle studied, and further that pressure failure will only result from frictive damage generated in the shoulder contact during handling, the internal pressure strength distributions shown in figure 16 were obtained using the computer model for the specified conditions of 0, 1, 3, 5, 10, 20 and 25 trips through a simulated filling line. It can be seen from that latter figure that a limiting pressure strength distribution is approached. Mean and minimum pressure strengths continue to decrease with increasing simulated trippage as well. This is indicative of the fact that while the numbers of localized frictive damage sites may be increasing with successive trips through the filling line, the strength determining depths of the frictive damage simulated by the model are reaching limiting depths. Consequently, the predicted internal pressure strengths approach limiting values, as well. Similar approaches to limiting pressure strengths with increasing bottle trippage are typically observed in practice.

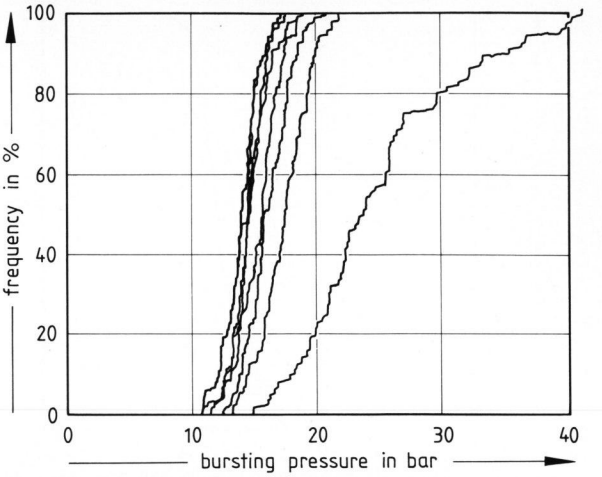

Figure 16. Internal pressure strength distributions for 33 cl bottle resulting from 0, 1, 3, 5, 10, 20 and 25 simulated trips through a filling line.

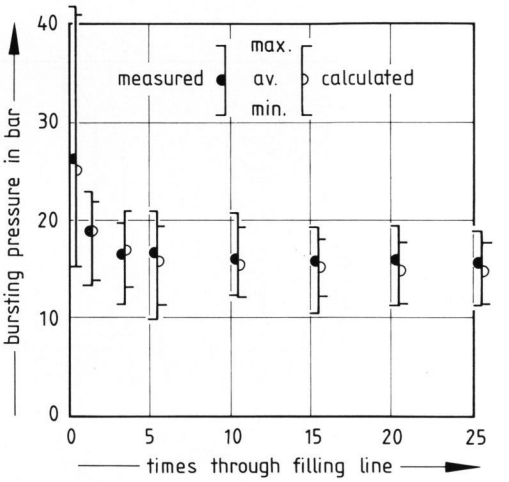

Figure 17. Measured and predicted mean, minimum and maximum internal pressure strengths for a 33 cl uncoated refillable bottle as functions of simulated filling line trippage.

The predictive model can then be used to predict the decreases in internal pressure strengths and the range of variation in those pressure strengths for a specified number of trips of a given bottle design through a filling line, as well as for the limiting strength case. Figure 17 shows the predicted mean, minimum and maximum internal pressure strength values compared with the actual corresponding measured pressure strength values for bottles subjected to actual filling line abuse. The pressure

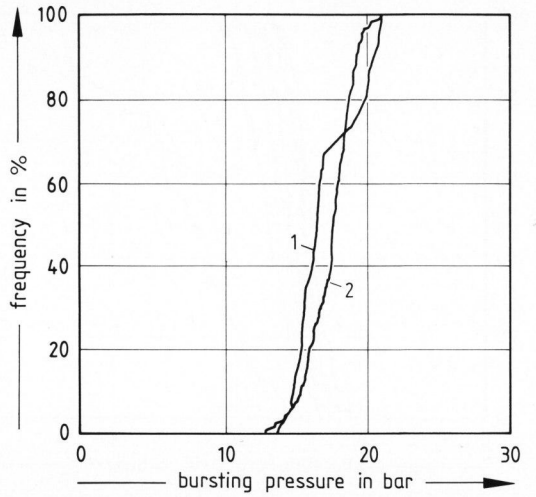

Figure 18. Measured and predicted internal pressure strength distributions for 15 33 cl uncoated refillable bottles subjected to a 3 min wet and filling line simulation treatment. Curve 1: measured (15 bottles), curve 2: simulated (100 bottles).

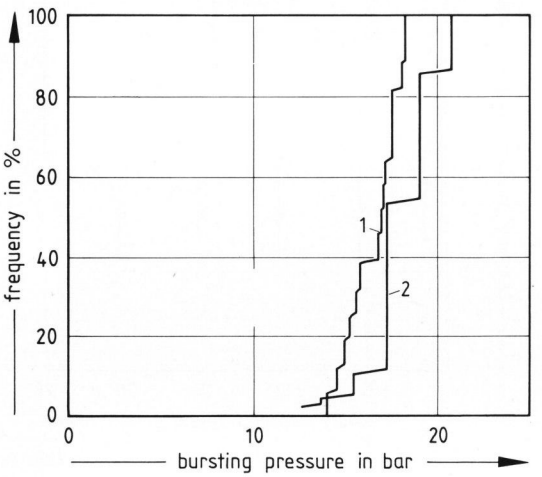

Figure 19. Measured and predicted internal pressure strength distributions for 50 33 cl uncoated refillable bottles subjected to a 3 min wet and filling line simulation treatment. Curve 1: calculated, curve 2: measured (50 bottles).

strengths were seen to decrease sharply on the first few initial trips through the filling line, as frictive damage was generated on otherwise virgin bottle surfaces. The mean internal pressure strengths decreased to a limiting value, due to the fact that, for the given frictive loading situation, as the frictive damage becomes more numerous in extent, the frictive damage produced is no deeper than a value determined for the particular loading conditions being experienced. Also, locations on the bottle surface having values of wall thickness at or near the minimum value become more probable of being frictively damaged as the number of trips increases.

The variability in the pressure strength data was seen to be high during the initial trippage, due to the large variability inherent in the severity or depth of damage present on the as-manufactured bottle surfaces. That variability decreased with increasing trippage as the maximum depth or severity of the frictive damage saturated with an increasing number of trips. The agreement between the predicted and actual measured values can be seen to be good with respect to the decrease in both pressure strength and the variability of the pressure strength data.

A second experiment was run in which the same bottles were abused using an AGR line simulator. The line simulator is a device in which a series of full or empty bottles are caused to move around a revolving table in wet or dry contact with one another and also with a variety of materials commonly used to guide bottles through filling lines. Twenty bottles were sampled, with thickness distributions being obtained for each bottle. The statistical parameters describing the wall thickness distributions were determined, and the full bottles were then exposed to a three minute line simulation treatment in a wet condition.

Following an aging period, fifteen of the line simulated bottles were then pressure-tested to destruction in an AGR ramp pressure tester. The remaining unbroken bottles were then used to determine the number of surface discontinuities and crescent crack width and number distributions in each segment.

An internal pressure strength distribution was predicted for 100 similar bottles using the computer model. That predicted distribution was compared with an actual experimental pressure strength distribution for the above 15 line simulated bottles as seen in figure 18. Agreement between the two distributions was seen to be good, again, as evidenced by the similarity in the relative positions and shapes of the two distributions.

The above procedure was repeated using 56 bottles, of the same bottle style and wall thickness distribution parameters, also exposed to a three minute line simulation using filled bottles and in a wet condition. Fifty of those bottles were aged and pressure-tested to destruction. The surface discontinuity distributions were determined for the remaining bottles, and the corresponding parameters calculated, using the wall thickness variation parameters measured earlier on the above mentioned fifteen bottles. The resulting predicted and measured internal pressure strength distributions are shown in figure 19. The agreement in mean pressure strengths and variability can be seen again to be quite good.

9. Summary

The present model, as applied to refillable pressure ware, requires accurate and time consuming measurements of glass wall thicknesses and surface discontinuity distributions, knowledge of the rela-

tionship between applied loads and the resulting stresses generated in the structure, and the nature of the relationship between surface discontinuity size and fracture stress to obtain accurate predictions of the resultant internal pressure strength distributions.

At present, the computer model described herein may not be reliably used to predict internal pressure strength distributions in lightweight nonrefillable pressure ware. However, the basic principles outlined in this paper will be of use in such predictions when continuing improvements in the bottle manufacturing process provide lessened variability in wall thickness and surface discontinuity distributions, and the relationships between the different types of possible surface discontinuities and failure stresses are better established. Additional studies of the effects of different processes on resultant wall thickness distributions are also needed.

The predictive model offers potential use as both a tool and a method to obtain a better understanding of and improvements in future lightweighted glass container strength distributions.

The authors wish to jointly acknowledge the managements of their respective organizations, GTA, the PLM Glass Research and Development Department of PLM at Hammar (Sweden) and American Glass Research, Inc. of Butler, PA for permission to publish the work contained within this study.

The authors would also like to acknowledge the words of an unknown Scandinavian physicist who said, freely translated: "Anyone would have done it in a different way. Several would have done it better. I did it my way. And if I had not done it, perhaps it would not have been done at all."

10. Reference

[1] Augustsson, B. O.: Changes in surface structure of glass from sliding contact. Glastek. Tidskr. **36** (1981) no. 2/3, p. 23–29. [Rev. Glastech. Ber. **55** (1982) no. 6, 82R1268.]

86R0375